



Studies of di-gamma and di-electron pairs in forward region of CMS detector

Artur Vasilyev (Moscow State University, Russia)

Supervised by:

Vardan Khachatryan (Alikhanyan National Scientific Laboratory (ANSL),
Armenia)

Ekaterina Kuznetsova (DESY Hamburg, Germany)

September 4, 2012

Abstract

This report presents calibration of CASTOR calorimeter of the CMS detector, using Hadron Forward calorimeter. For this purpose, pp Minimum Bias events at $\sqrt{s} = 900$ GeV and 7 TeV were generated on Pythia6 by Monte Carlo method. From these samples di-electron and di-gamma pairs had been selected. After that invariant mass distributions of ee and $\gamma\gamma$ pairs had been created and analyzed.

Also there is a possibility to take data (detector level) at $\sqrt{s} = 5$ TeV in 2013, that's why we generated MB events at such center of mass energy.

Content

1. Introduction
2. CMS detector
 - a) CASTOR calorimeter
 - b) Hadron Forward (HF) calorimeter
3. CASTOR calibration
4. Results
5. Conclusion
6. References

Introduction.

- Our aim is the absolute calibration of CASTOR calorimeter of CMS detector with $e+e$ or $\gamma+\gamma$ pairs
- Particle decays can be used for the calibration by analyzing the decay products and their invariant mass spectrum

CMS detector.

The Compact Muon Solenoid (CMS) [1] experiment is one of two large general-purpose particle physics detectors built on the proton-proton Large Hadron Collider (LHC) at CERN.

CMS is designed as a general-purpose detector, capable of studying many aspects of proton collisions at 14 TeV, the center-of-mass energy of the LHC particle accelerator. It contains subsystems which are designed to measure the energy and momentum of photons, electrons, muons, and other products of the collisions. The innermost layer is a silicon-based tracker. Surrounding it is a scintillating crystal electromagnetic calorimeter, which is itself surrounded with a sampling calorimeter for hadrons. The tracker and the calorimetry are compact enough to fit inside the CM Solenoid which generates a powerful magnetic field of 3.8 T. Outside the magnet are the large muon detectors, which are inside the return yoke of the magnet.

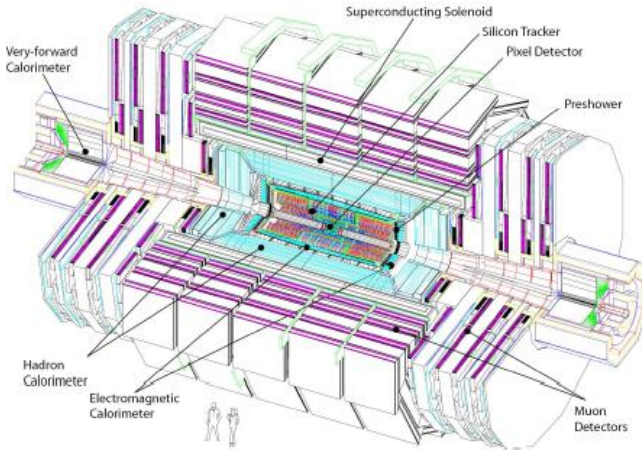


fig.1 The set up of the CMS.

The coordinate system adopted by CMS has the origin centered at the nominal collision point inside the experiment, the y -axis pointing vertically upward, and the x -axis pointing radially towards the center of the LHC. Thus, the z -axis points along the beam direction towards the Jura mountains from LHC Point 5. The azimuthal angle ϕ is measured from the x -axis in the x - y plane. The polar angle θ is measured from the z -axis. Pseudorapidity is defined as

$$\eta = -\ln \tan(\theta/2). \quad (1)$$

The central feature of the Compact Muon Solenoid (CMS) apparatus is a superconducting solenoid of 6 m internal diameter. Within the field volume are the silicon pixel and strip tracker, the crystal electromagnetic calorimeter (ECAL) and the brass/scintillator hadron calorimeter (HCAL) Muons are measured in gas-ionization detectors embedded in the steel return yoke. In addition to the barrel and endcap detectors, CMS has extensive forward calorimetry. The most forward station of HCAL, Hadronic Forward (HF) calorimeter, covers $3.0 < |\eta| < 5.0$. CASTOR calorimeter, located at one side of the CMS, covers $-6.6 < \eta < -5.2$.

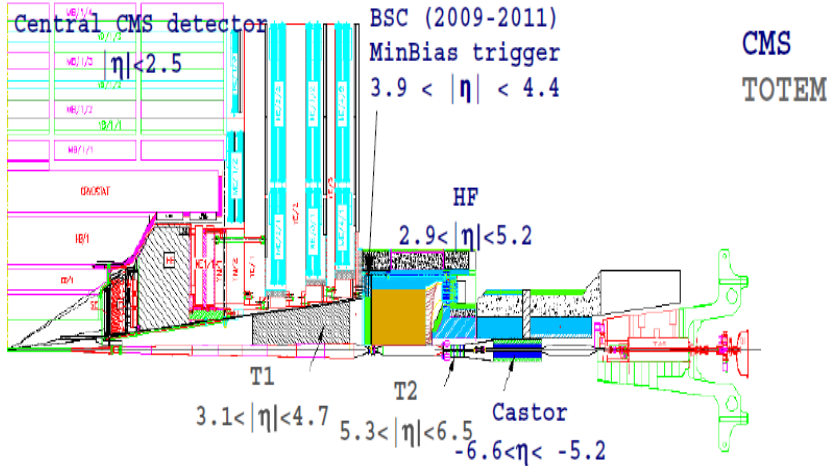


fig.2 More detailed view of forward region of the CMS detector.

CASTOR calorimeter.

The CASTOR (Centauro And STrange Object Research)[2] detector is located at a distance of 14.4 m from the CMS interaction point right behind the Hadronic Forward (HF) calorimeter, covering the pseudorapidity region $-6.6 < \eta < -5.2$. This is a quartz-tungsten Cerenkov sampling calorimeter. That is, it is made of repeating layers (arranged in a sandwich structure) of quartz and tungsten plates. The former is used as active material because of its radiation hardness, while the latter serves as the absorber medium providing the smallest possible shower size. The signal in CASTOR is produced when charged shower particles pass through the quartz plates with the energy above the Cerenkov threshold (190 keV for electrons). The generated Cerenkov light is then collected by air-code light guides, which are transmitting it further to photo-multipliers tubes (PMTs). These devices produce signals proportional to the amount of photons detected. As can be seen in Figure 1, the detector plates are tilted at 45° w.r.t. the beam axis to maximize the Cerenkov light output in the quartz. The CASTOR calorimeter is a compact calorimeter with the physical size of about 65 cm×36 cm×150 cm and having no radial segmentation in.

CASTOR is segmented in 16 azimuthal sectors. The longitudinal segmentation is done in 14 so-called modules and separate electromagnetic (e, γ) and hadronic (jets) showers and search for phenomena with anomalous hadronic energy depositions. The total length of CASTOR corresponds to about 10 radiation length, while first EM modules have ~20 radiation length.

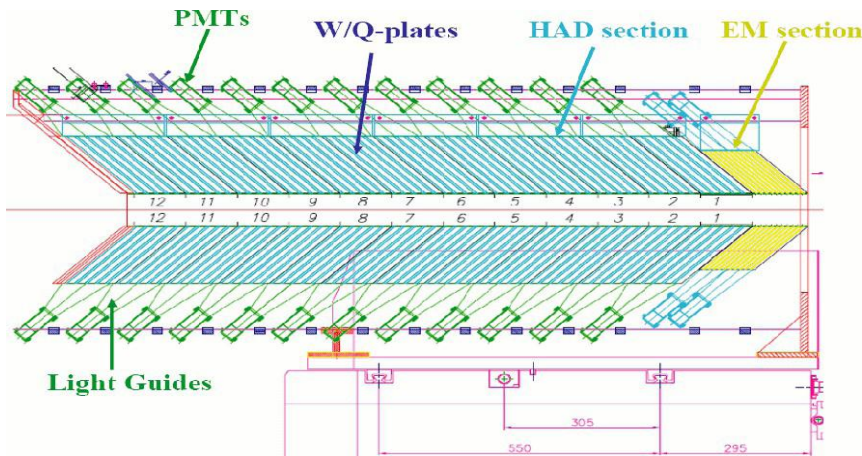
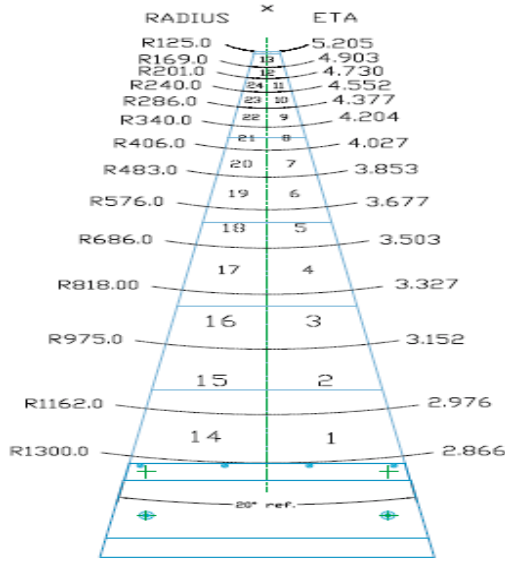


fig. 3.CASTOR longitudinal Scheme.

Hadron Forward calorimeter (HF).



Ring	(r_{in}, r_{out}) [mm]	$\Delta\eta$	$\Delta\phi$ [degree]
1	(1162–1300)	0.111	10
2	(975–1162)	0.175	10
3	(818–975)	0.175	10
4	(686–818)	0.175	10
5	(576–686)	0.175	10
6	(483–576)	0.175	10
7	(406–483)	0.175	10
8	(340–406)	0.175	10
9	(286–340)	0.175	10
10	(240–286)	0.175	10
11	(201–240)	0.175	10
12	(169–201)	0.175	20
13	(125–169)	0.300	20

Fig.4. The transverse segmentation is 0.175×0.175 in $\Delta\eta \times \Delta\phi$ with the exception of two towers (12 and 13) at the tip of the wedge near the beam pipe.

The hadron forward calorimeter (HF)[3] covers the pseudorapidity range $3.0 < |\eta| < 5.0$. It's located from both sides of IP at the distance $z = \pm 11.1$ m. It has tower structure. This structure is azimuthally subdivided into 20-degree modular wedges. Thirty-six such wedges (18 on either side of the interaction point) make up the HF calorimeters

CASTOR calibration.

Why from all the data we selected only electrons or gamma? Because we have Electro Magnetic calorimeters : HF and CASTOR, which can detect electrons, positrons and gammas. We want to reconstruct particles, which created electron and gamma pairs. We already know the masses of these mesons, they are for example: π^0, η decay into $2e$ or 2γ ; $\rho, \omega, \eta', \phi, J/\Psi$ decay into $2e$. So in the invariant mass spectrum we can see these resonances.

Suppose that in the reaction of the particle X decays into N different particles. In this case, each particle detected and recorded for each measured momentum and energy. Using the laws of conservation of energy and momentum, we can reconstruct the invariant mass (rest mass) M particles X, registering its decay products:

$$M_{inv}(X) = \sqrt{(\sum_{i=1}^N E_i)^2 - (\sum_{i=1}^N p_i)^2} \quad (2)$$

Where E and p are energy and impulse of the product of the decay. In our case we have N=2. One e/gamma is detected by CASTOR and another e/gamma is detected by HF.

Our aim is to absolute calibrate CASTOR detector using HF. The aim of the absolute calibration is to measure which energy deposit in the calorimeter, in units of GeV, results in a specific output of the electronics measured in fC (femtoCoulomb).

For the absolute calibration there exist several independent options. Particle decays can be used for absolute calibration by analyzing the decay products and their invariant mass spectrum. So, we have to find out energy coefficient k_{CAS} of CASTOR, which translates energy and momentum from arbitrary units to GeV scale.

$$E[\text{GeV}] = k_{CAS} * E[\text{a.u.}] \quad (3)$$

$$p[\text{GeV}/c] = k_{CAS} * p[\text{a.u.}] \quad (4)$$

Energy in arbitrary units can be written as:

$$E[\text{a.u.}] = \sum_i \alpha_i * E_i [fC] \quad (5)$$

Where α_i is a coefficient, which takes into account nonuniformity of individual calorimeter channels.

In case rest mass $m \ll E1, E2$ we can write invariant mass as:

$$m = \sqrt{E1 * E2 - p1 * p2 * \cos(\varphi1 - \varphi2) + ctg\theta1 * ctg\theta2}, \quad (6)$$

where

m - rest mass of the mother particle,

$E1, E2$ - energies of decay products

$p1, p2$ - momentum of decay products

$\varphi1, \varphi2$ -azimuthal angles of decay products

$\theta1, \theta2$ -acceptance of decay products

$$ctg\theta1 = \frac{1 - \exp(-2*\eta1)}{2 * \exp(-\eta1)} \quad (7)$$

$$ctg\theta2 = \frac{1 - \exp(-2*\eta2)}{2 * \exp(-\eta2)} \quad (8)$$

And for $p1$ we can write:

$$p1 = E1 * \sin(\theta1) \quad (9)$$

$$\text{here } \theta1 = 2 * \text{atan}(\exp(-\eta1)) \quad (10)$$

As a result, in formula (6) we have E, η, φ variables. We measure all these variables for HF. In case of CASTOR we have only E and φ , and for η we take mean value for example 5.8.

If we know rest mass of mother particle m , using formulas (3) -(10), we can find out calibration coefficient k_{CAS} .

My studies devoted to CASTOR calibration feasibility using mesons ($\eta, \varphi, J/\Psi...$) decaying into $e+e$ or $\gamma+\gamma$ pairs. Due to the small masses of these mesons the decay angles are typically very small at large energies and therefore the final state detection could be done using CASTOR and HF calorimeters.

Results.

In our work we analyse generated about 2 billion Minimum Bias* events of pp-collisions at the center-of-mass energy of 7 TeV, 5 TeV and 400 million events for 900 GeV. Among these events we selected electron, positron and gamma particles. After that we wrote a program, which was analyzing these particles, included in Python files. And our program plotted the histograms of invariant mass, pseudo-rapidity, energy distributions.

We have already data of pp-collision at a center of mass $\sqrt{s} = 900$ GeV and 7 TeV which were taken during 2009-2011 years. These data was collected without selecting if it is electron or gamma. Statistics was 2 billion MinBias events. We have analysed this data and got invariant mass distributions of ee and $\gamma\gamma$ events in HF and CASTOR calorimeters. Lower I'll show them.

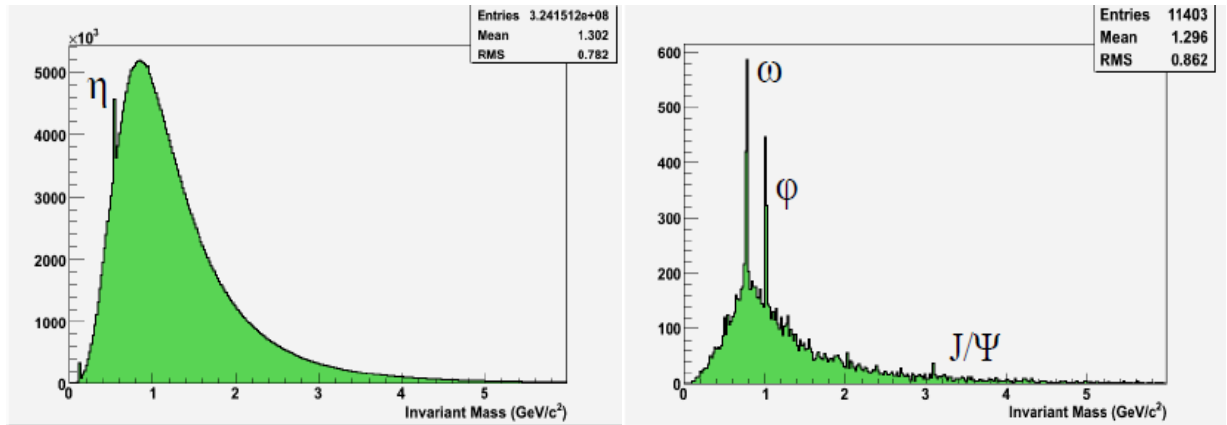


Fig.7. Invariant mass distribution of $\gamma\gamma$ (left) and ee (right) pairs in HF and CASTOR detectors ($\sqrt{s} = 7$ TeV).

We can see resonances on the invariant mass distributions. η meson consists of correlated $\gamma\gamma$ pairs and ω , ϕ , J/Ψ consist of correlated ee pairs. Background consist of non-correlated ee or $\gamma\gamma$ pairs. Also we can see that $\gamma\gamma$ events have 10^8 entries and ee events have 10^4 entries. It means that $\gamma\gamma$ events are higher than ee events and we won't see resonances of ee pair in $\gamma\gamma$ plot.

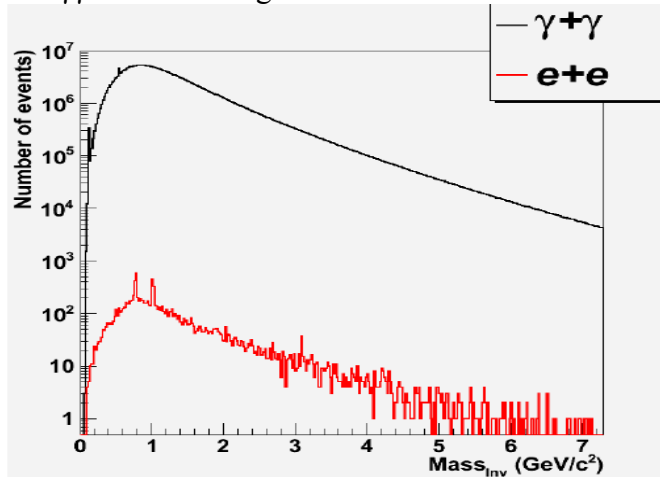


Fig.8. Invariant mass distribution in logarithmic scale of $\gamma\gamma$ and ee pairs in HF and CASTOR detectors ($\sqrt{s} = 7$ TeV).

¹ Minimum Bias* - the definition of MB events is experimental (no theory!): $\sigma_{\text{meas}} = f_{\text{sd}} \cdot \sigma_{\text{sd}} + f_{\text{dd}} \cdot \sigma_{\text{dd}} + f_{\text{nd}} \cdot \sigma_{\text{nd}}$ where the f_i are the acceptances, dependent on the detectors and triggers. (sd-single diffractive, dd-double diffractive, nd-nondiffractive). Therefore MB can be defined as INELASTIC collisions of two protons accepted by the trigger with the only requirement being some

We can do some conclusion from fig.8. HF and CASTOR calorimeters can measure energy and momentum of the incoming particle, but they cannot distinguish charged particles. If we have some instrument which can distinguish charge of a particle, we'll have red invariant mass distribution. If we don't have such an instrument, we will have black spectrum and we'll calibrate CASTOR detector with η meson.

So as we have $\gamma\gamma$ events more than 10^4 times than ee events, that is there is no point to look ee events and we concentrate on $\gamma\gamma$ events. Let's see distributions of $\gamma\gamma$ events at $\sqrt{s} = 900$ GeV.

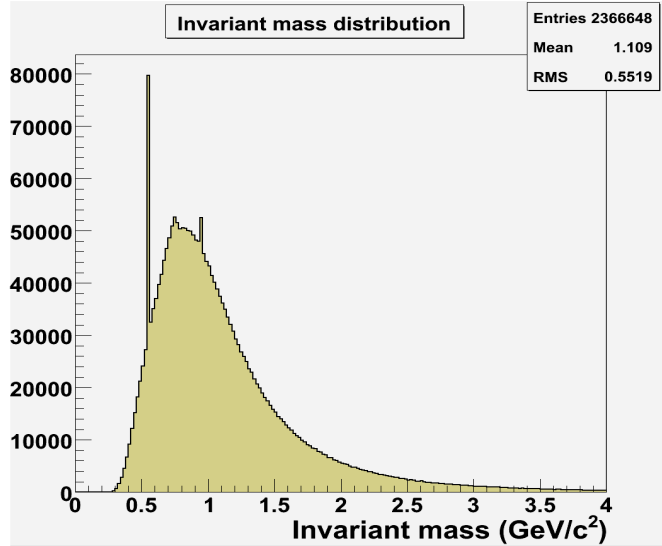


Fig.9. Invariant mass distribution of $\gamma\gamma$ pairs in HF and CASTOR detectors ($\sqrt{s} = 900$ GeV). MinBias=400 million events.

Also we wanted to see clear distributions without non-correlated $\gamma\gamma$ pairs. And we put some isolating conditions, while selecting electrons or gamma. We assume that there is no higher than 1 GeV particle in the neighboring segment in CASTOR and selected cluster in HF detector.

These regions are the next:

For HF: $[\eta - 0.35, \eta + 0.35]$ and $[\phi - 25, \phi + 25]$ region

For CASTOR: $-6.4 < \eta < -5.4$ and $[\phi - 45, \phi + 45]$ region

I want to note that real borders for CASTOR are $-6.6 < \eta < -5.2$. And for HF: $-5.0 < \eta < -3.0$. But we retreated from the border and put next values: -5 is changed to -4.8, -6.6 changed to -6.4, -5.2 changed to -5.4. We did it, because we cannot create clusters on the border. And there is also another reason, which won't be discussed here.

Of course, these conditions are the approximate description of absence of 1 GeV particle. For CASTOR there is an interesting case, which have to be considered.

In the normal situation, if one e/γ with energy higher than 30 GeV hits detector, only one sector will give signal and neighboring segments will give nothing. If e/γ hits exactly between two sectors, than we will get signal from these two sectors and neighboring segments to these two segments will give nothing.

And after putting isolating conditions we get these histogram:

activity in the detector, i.e. a minimal p_T threshold of ≈ 100 MeV (ISR-experiments, UA5, E735, CDF). (No energy threshold \Rightarrow no bias).

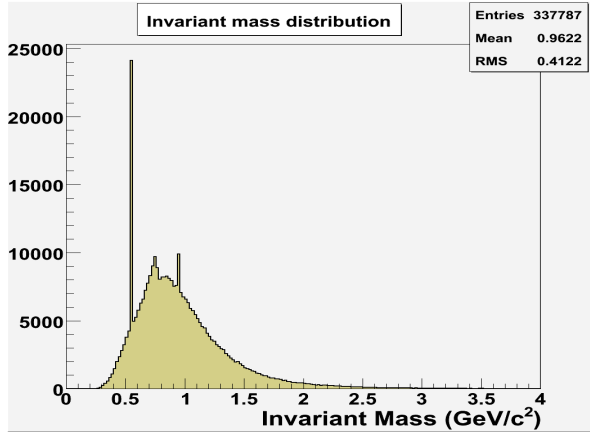


Fig.10. Invariant mass distribution (with isolation) of $\gamma\gamma$ pairs in HF and CASTOR detectors ($\sqrt{s} = 900$ GeV).

And we see that background become smaller and we see mesons better.

In the future there is a likely possibility that we'll have detector TOTEM, which can distinguish charged particles. And this experiment will operate at $\sqrt{s} = 5$ TeV. So we also did some calculation what we will see. 2 billion MinBias events were generated and we got next plot:

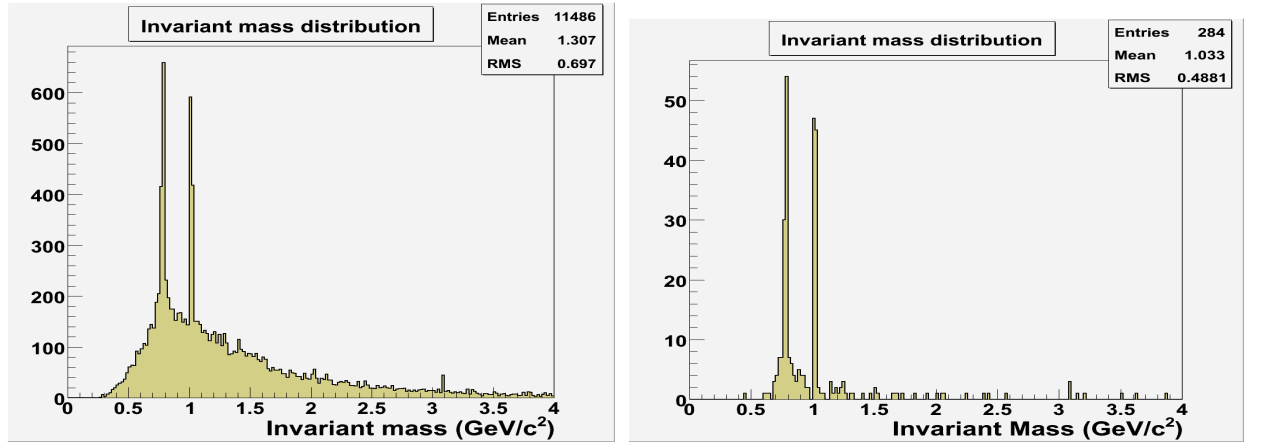


Fig.11. Invariant mass distribution (without isolation-left, with isolation-right) of ee pairs in HF and CASTOR detectors ($\sqrt{s} = 5$ TeV).

Also we analyzed situation when both electrons are detected by CASTOR calorimeter :

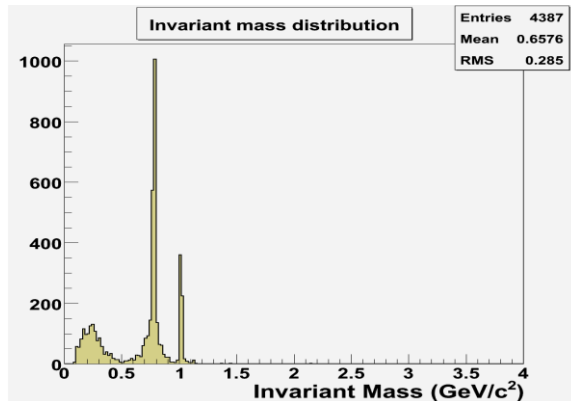


Fig.12. Invariant mass distribution (without isolation) of ee pairs in CASTOR and CASTOR detectors ($\sqrt{s} = 5$ TeV).

Also we get energy distributions of ee and $\gamma\gamma$. There was 30 GeV energy cut. It means that we select electrons and gamma with energy higher than 30 GeV. Most of the pictures are almost the same, so we'll discuss only one.

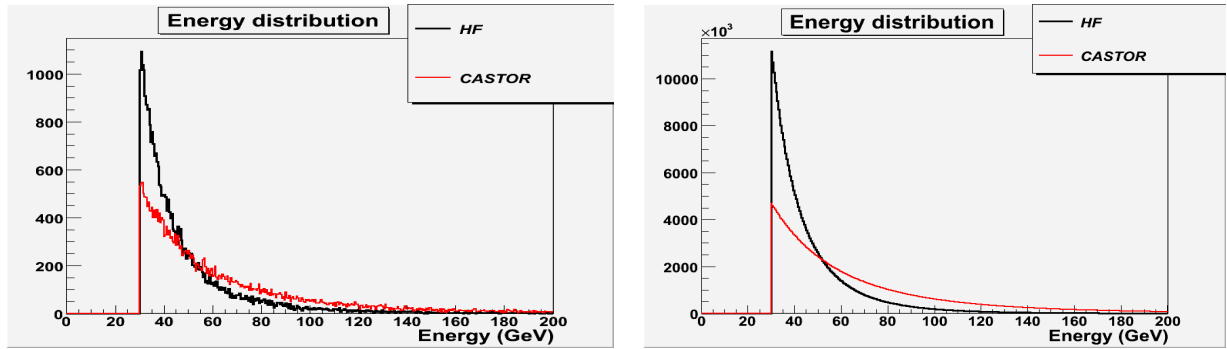


Fig.13. Energy distributions of ee (left) and $\gamma\gamma$ (right) pairs in HF and CASTOR detectors ($\sqrt{s} = 7$ TeV).

So in fig.13 we see energy distribution of ee and $\gamma\gamma$ pairs. We have to notice that these distributions are not same in CASTOR and HF calorimeters. And if we, for example, have 60 GeV energy-cut, we'll lose a lot of statistics. Further I'll show another plots:

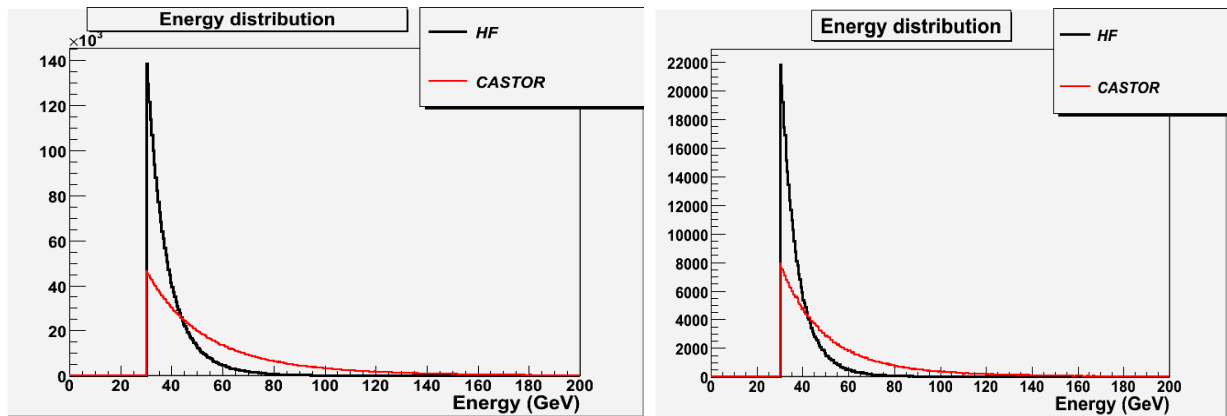


Fig.14 Energy distributions of $\gamma\gamma$ without isolation(left) and with isolation (right) pairs in HF and CASTOR detectors ($\sqrt{s} = 900$ GeV).

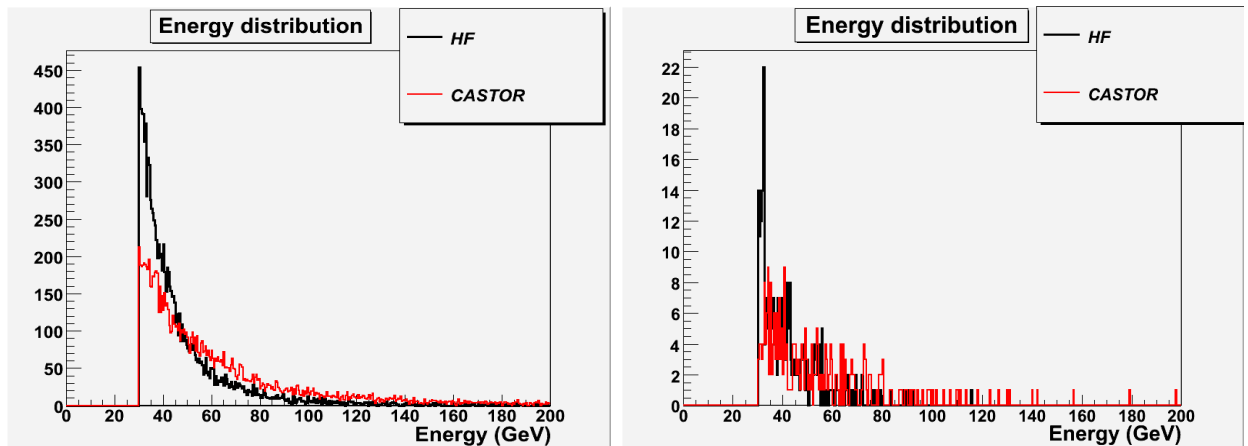


Fig.15 Energy distributions of ee without isolation(left) and with isolation (right) pairs in HF and CASTOR detectors ($\sqrt{s} = 5$ TeV).

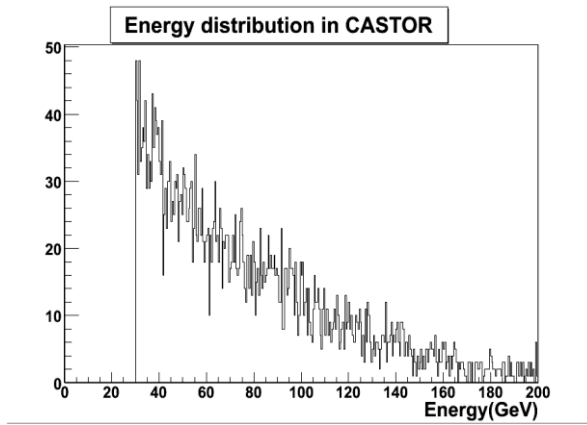


Fig.16. Energy distributions of ee without isolation pairs in CASTOR and CASTOR detectors ($\sqrt{s} = 5$ TeV).

Let's also discuss pseudorapidity distributions in HF and CASTOR. The coverage of pseudorapidity of HF is $3.0 < |\eta| < 5.0$, and for CASTOR is $-6.6 < \eta < -5.2$.

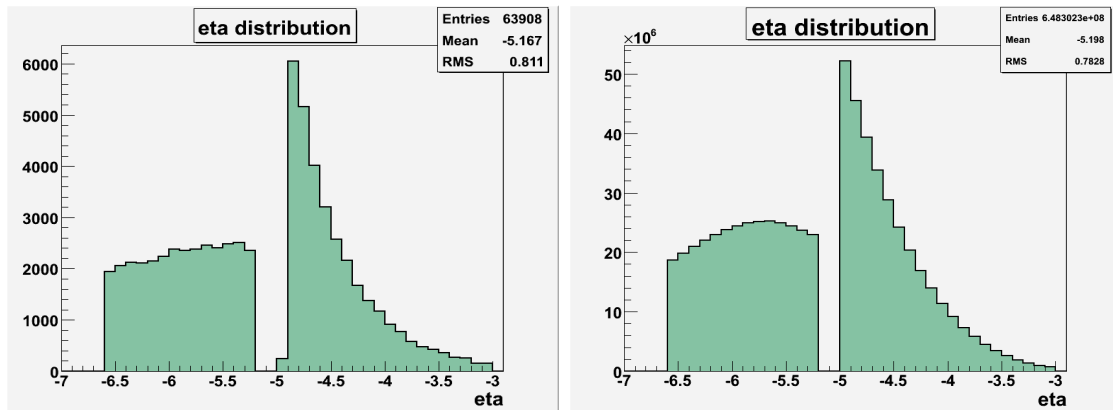


Fig.13. pseudorapidity distributions of ee (left) and $\gamma\gamma$ (right) pairs in HF and CASTOR detectors ($\sqrt{s} = 7$ TeV).

Of course, there is a question: "Why HF is higher than CASTOR?". To answer this question I'll show a piece of code:

```
for( int i=0; i<eta1.size(); i++ )
for( int j=0; j<eta2.size(); j++ )
{
    eCand_Eta_Gen->Fill(eta1[i]);
    eCand_Eta_Gen->Fill(eta2[j]);
}
```


Here you can see, that if we have 1 e or gamma in HF , it can make more than 1 pair with e/ γ in CASTOR. If we assume that 1 particle makes only 1 pair with another particle from another detector, we'll get the next distribution:

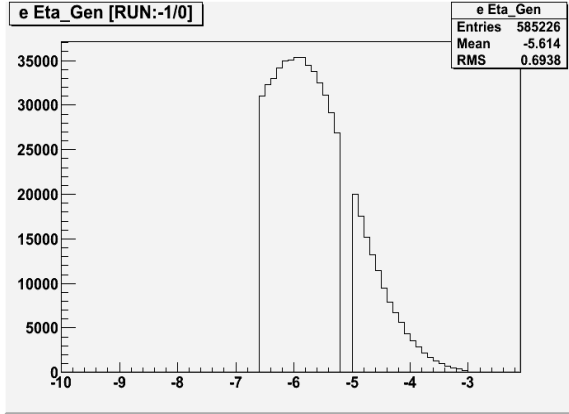


Fig.13. pseudorapidity distributions of $\gamma\gamma$ pairs in HF and CASTOR detectors ($\sqrt{s}=7$ TeV).

Let's see another pseudorapidity distributions:

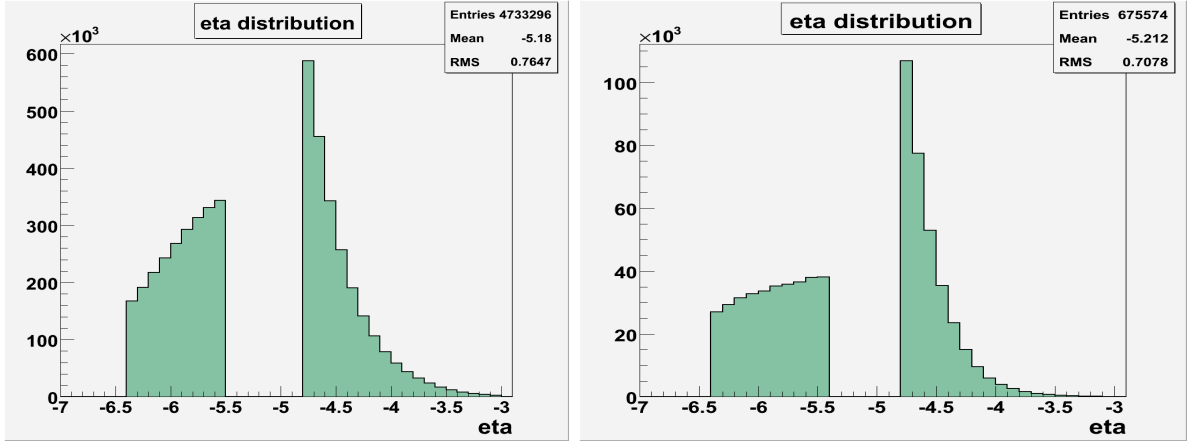


Fig.13. pseudorapidity distributions of $\gamma\gamma$ without isolation (left) and with isolation(right) pairs in HF and CASTOR detectors ($\sqrt{s}=900$ GeV).

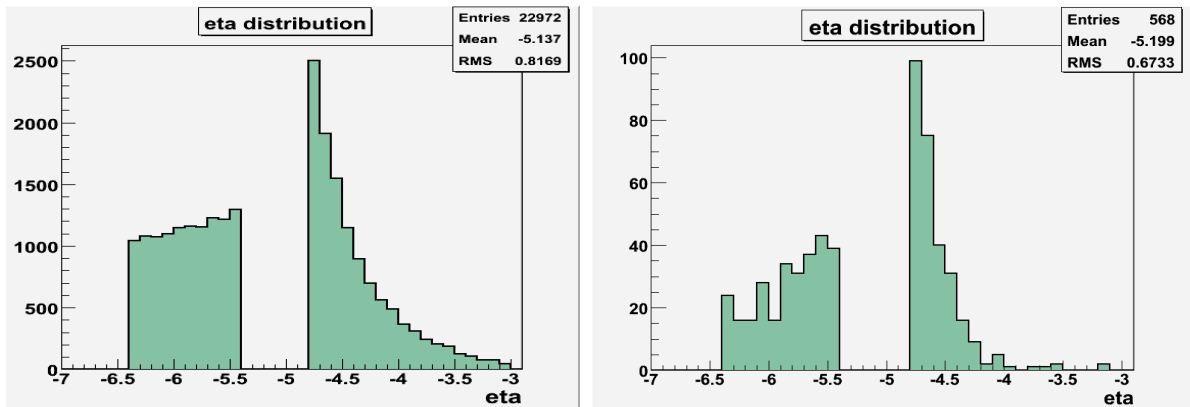


Fig.14. pseudorapidity distributions of ee pairs without isolation (left) and with isolation(right) in HF and CASTOR detectors ($\sqrt{s}=5$ TeV).

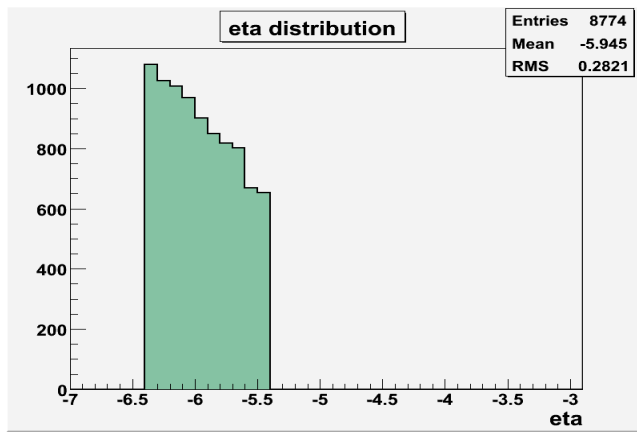


Fig.15. pseudorapidity distribution of ee pairs with isolation in CASTOR and CASTOR detectors ($\sqrt{s}=5$ TeV).

Conclusion.

- Calibration of CASTOR calorimeter is challenging and requires high statistics
- Due to high contribution of $\gamma\gamma$ events, ee events can be used only in the case of good electron identification (TOTEM)
- Amount of non-correlated gamma grows with energy, that's why small energies are good for calibration with $\gamma\gamma$ events ($\sqrt{s}=900\text{GeV}$)

Reference.

- [1] CMS Physics Technical Design Report Volume I: Detector Performance and Software
- [2] Ekaterina Kuznetsova, Performance and calibration of CASTOR calorimeter at CMS, CMS CR -2011/199, v2, 11 October 2011.
- [3] Eur. Phys. J. C 53, 139–166 (2008)